A&A 447, 1145–1151 (2006)
DOI: 10.1051/0004-6361:20053929
© ESO 2006

Astronomy & Astrophysics

Astrometric observations of Phobos and Deimos with the SRC on Mars Express

J. Oberst[1], K. D. Matz[1], T. Roatsch[1], B. Giese[1], H. Hoffmann[1], T. Duxbury[2], and G. Neukum[3]

[1] German Aerospace Center (DLR), Institute of Planetary Research, Rutherfordstr. 2, 12489 Berlin, Germany
e-mail: Juergen.Oberst@dlr.de
[2] Jet Propulsion Laboratory, Pasadena, California, USA
[3] Freie Universität Berlin, Germany

Received 27 July 2005 / Accepted 7 October 2005

ABSTRACT

Observations of Phobos and Deimos, carried out by the SRC (Super Resolution Channel) on the Mars Express spacecraft between May 2004–April 2005, were used to determine the center-of-figure positions of the two Satellites with accuracies of 0.5–5 km (Phobos) and 1.0 km (Deimos). We find that the Phobos and Deimos orbit predictions from NASA-JPL (Jet Propulsion Laboratory) and ESA-ESOC (European Space Operation Center) differ substantially among each other and also do not agree with the actually observed positions of the satellites. Hence, our new astrometric data may motivate new efforts for Phobos and Deimos orbit modeling.

Key words. astrometry – ephemerides – planets and satellites: individual: phobos – planets ans satellites: individual: Deimos

1. Introduction

Phobos and Deimos, the two natural satellites of Mars were discovered in 1877 by Asaph Hall, an astronomer at the United States Naval Observatory. There is great interest in the long-term motion of the two satellites in the gravity field of the planet. In particular, the tidal acceleration of Phobos may reveal constraints on the anelastic properties of the Martian interior, and ultimately on the planets composition and thermal evolution. The orbital motion of the satellites is being studied by ground-based observations up to the present day (Morley 1989; Lainey et al. 2005). During Mars oppositions positional accuracies on the order of several kilometers can be achieved. From image data obtained by Mariner 9 (1971–1972), Phobos positions were determined at an accuracy of 3–10 km (Duxbury & Callahan 1989). Similar positional data were achieved by analysis of the Viking Orbiter images (Duxbury & Callahan 1988). During the ill-fated Soviet Phobos mission, operating for a limited time span of 2 months in 1989, the positions of Phobos were measured with an accuracy of approx. 2 km (Kolyuka et al. 1991). More than ten years after, the Mars Global Surveyor engaged in several flyby maneuvers of Phobos. Laser ranging measurements to Phobos (Banerdt et al. 1999) and positional measurements of the Phobos shadow on the surface of Mars (Neumann et al. 2004; Bills et al. 2005) were carried out. More recently, the cameras on the Mars Exploration rovers observed Phobos and Deimos transits across the solar disk (Bell et al. 2005). Surprisingly, the observed satellite positions did not agree with the various predictions, made on the basis of the early spacecraft image data, for reasons that are currently being discussed. Beginning in May 2004, Mars Express had a number of close encounters with Phobos. The onboard camera SRC (Super Resolution Channel) obtained a number of observations and also took images of Deimos from large range. In this paper, we report on these new measurements, and we discuss how these compare with the early satellite orbit predictions and the recent spacecraft observations.

2. Mars express mission and cameras

Mars Express is in an elliptic near-polar (86.6°) orbit, almost perpendicular to the near-equatorial and near-circular orbits of the two satellites. With an apoapsis of 13 560 km, the Mars Express trajectory reaches out well beyond the orbit of Phobos (9515 km), but falls short of the orbit of Deimos (23 500 km). As the ratios in orbit period of MEX and Phobos are similar, 7.5, vs. 7.65 h, there are typically multiple flybys in consecutive orbits (at similar orbit positions of the Phobos) followed by a period without Phobos encounters. Hence, the Phobos positions reported in this paper are unfortunately not evenly distributed along the Phobos orbit.

Mars Express is equipped with the HRSC (High Resolution Stereo Camera), a push-broom scanner, designed for multi-spectral mapping of the surface of Mars in 3-D (Neukum et al. 2005). In contrast, the SRC (Supper Resolution Channel) is a framing camera, equipped with a Maksutov-Cassegrain

Article published by EDP Sciences and available at http://www.edpsciences.org/aa or http://dx.doi.org/10.1051/0004-6361:20053929

Table 1. SRC camera parameters.

Parameter	Value
Focal length	974.5 mm[a]
F number	9.2
Detector array size	1024×1024
Pixel size	$9 \times 9\ \mu$m
FOV	0.543°
IFOV	1.9 arcsec

[a] Inflight measurement, Oberst et al. (2005).

telescopic lens, designed to show details within the large HRSC scenes (Table 1). Although the SRC is operated through the HRSC digital unit, it practically acts as a separate camera. Typically the panchromatic SRC images are obtained rapidly, in a sequence of 7 images. All results reported in this paper are derived from SRC images.

3. Astrometric measurements

Mars Express and the onboard cameras were not intended for astrometric observations of the Martian satellites. The spacecraft star sensor, mounted on the spacecraft platform opposite the camera, is usually looking at the surface of Mars during the Phobos flybys and therefore unable to support the imaging. Hence, during the flybys, the camera pointing is solely controlled by the onboard reaction wheels. Also, the exposure times of the SRC images of Phobos and Deimos are typically very short (20–50 ms) to avoid saturation. Consequently, no stars are visible in these images for the verification of camera pointing. However, a few stars were captured in dedicated long-exposure images, taken immediately before and (sometimes) after the flyby sequences. During 12 individual flybys, Phobos was observed from ranges between 4000 km and 150 km at solar phase angles between 23 and 84. In contrast, Deimos was observed on three occasions from ranges near 11 000 km (Table 2, Fig. 1). During a flyby, the camera is pointed at some fixed (inertial) position in the celestial sphere, and an SRC imaging sequence is executed as the target crosses the field of view. Among the typical set of 7 images, only 2–4 images would show Phobos or parts thereof. During two of the flybys (see Table 2), observations were carried out by slewing the camera (i.e., by turning the spacecraft) across the target. Measurements of the Phobos and Deimos center of figure (Phobos radii: $13.4 \times 11.2 \times 9.2$ km; Deimos radii: $7.5 \times 6.1 \times 5.2$ km; Seidelmann et al. 2002) were obtained by fitting the limb and terminator (both assumed to be ellipsoidal) to the observations, using an interactive software tool (see Fig. 2). In those images that show only parts of Phobos, only crude measurements of the Phobos center position were possible (see Fig. 2).

4. Results

We have measured the Phobos and Deimos center-of-figure positions in 36 SRC images. We provide listings of the raw image

Table 2. Mars Express orbits and satellite flybys.

Orbit No	Encounter time UTC	True anomaly, deg	Flyby distance, km
Phobos:			
413	2004-05-18T08:34	37.7	1883
649	2004-07-23T12:40	184.4	1836 *
682	2004-08-01T18:35	178.5	1469
715	2004-08-11T00:30	172.5	1213
748	2004-08-20T06:25	167.0	1247
756	2004-08-22T12:06	170.6	149 *, **
1064	2004-11-16T14:22	121.5	4676
1163	2004-12-14T08:06	102.9	3835
1212	2004-12-28T01:18	101.0	1965 **
1558	2005-04-03T23:51	47.9	3598
1574	2005-04-08T11:21	63.1	3797
1607	2005-04-17T17:15	55.5	3977
Deimos:			
0973	2004-10-22T08:06	239.1	10 931
1010	2004-11-01T10:15	240.1	11 068
1222	2004-12-30T19:34	260.8	11 844

* Camera was slewed across target, all others: inertial pointing.
** No SRC images available from this orbit.

sample/line measurements of the Phobos center of figure, including errors (Table 3), and the computed position of Phobos and Deimos on the celestial sphere (Table 4) as seen from the position of the spacecraft (listed in Table 5). The errors of the computed sky positions can be attributed to three main sources (Duxbury & Callahan 1988, 1989), the interactive limb position measurements, the errors in the reported pointing of the camera, as well as the errors in the spacecraft positions. The errors in the limb position measurements were adopted to be 3 SRC pixels in the general case. Larger errors were assumed in those cases where only small parts of Phobos were visible (Table 3). The error of the Mars Express positions is reported to be on the order of 500 m with respect to Mars (ESOC flight dynamics team, pers. communication). This is confirmed by positional measurements of features on the surface of Mars by photogrammetric techniques (Scholten et al. 2005). Calibration sequences of bright stars, e.g. SPICAM show that the inertial pointing when controlled by reaction wheels is typically stable (over time scales relevant for a flyby) to within 5 SRC pixels. The position measurements carried out in orbit 682 and 1163 are the only ones, in which the nominal pointing data could be directly verified. Long exposure images were taken at the beginning and the end of the SRC sequence of orbit 1163. Three stars were identified in both these images. We could verify that the reported inertial pointing was correct and stable during the imaging sequence to within 5 pixels. On the other hand, a long exposure image was taken at the beginning of SRC sequence of orbit 682. Four stars were identified in this image (Fig. 3), and the nominal reported camera pointing was found to be in error by approx. 200 SRC pixels. As a consequence, we cannot rule out incidental gross outliers in the nominal pointing data. A comparison of the measured Phobos positions with the various predictions show more or less consistent shifts, suggesting

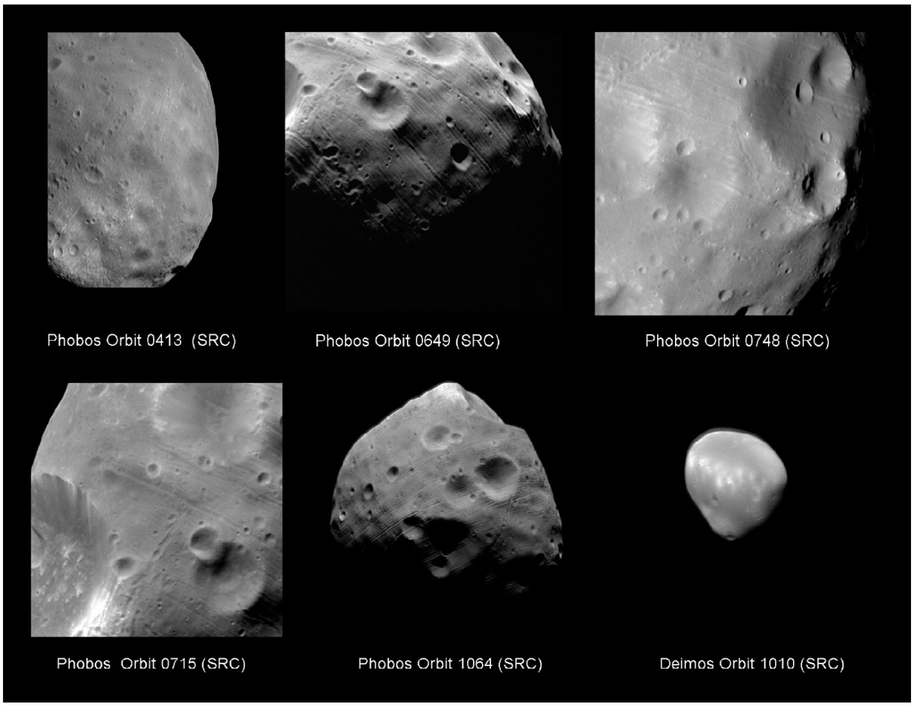

Fig. 1. Phobos and Deimos sample images obtained by SRC.

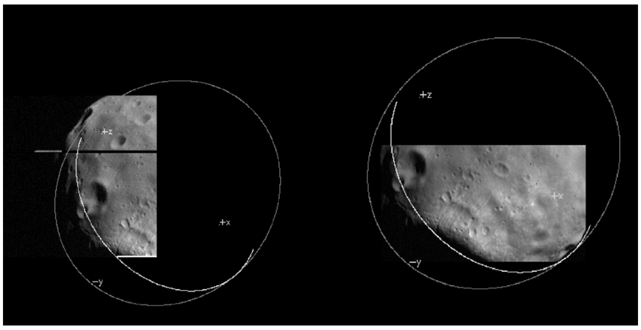

Fig. 2. Phobos SRC images and best limb and terminator fits.

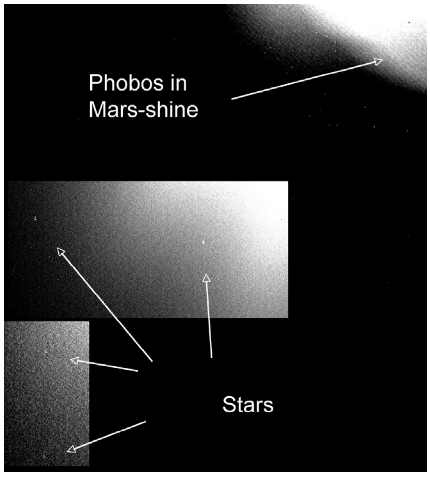

Fig. 3. Phobos SRC image from orbit 682 showing Phobos (upper right corner) and four stars (m = 7.3−9.1). Incidentally, only the dark hemisphere of Phobos, illuminated by sunlight reflected from the surface of Mars (Mars shine), was captured. The portion of the image where the stars are located is severely stretched.

that such outliers are not common. In the particular case of orbit 682, the Phobos positions reported in Table 3 were corrected for the known pointing error.

Defining the error due to the limb measurements to be σ_a, the pointing error to be σ_b, and the error in the spacecraft position to be σ_c, the total error σ is estimated to be (cf. Duxbury & Callahan 1988, 1989):

$$\sigma = \sqrt{\sigma_a^2 + \sigma_b^2 + \left(\arctan\left(\frac{\sigma_c}{r}\right)\right)^2} \quad (1)$$

where r is the range of the spacecraft from the target (Table 2). We find that the error totals of our measurements vary over a range between 15 arcsec in the best case and 200 arcsec when Phobos is observed from close range and – at the same time – limb fitting is poor (see Table 4, last column). This translates to a Phobos positional uncertainty perpendicular to the line-of-sight of 0.5–5.0 km. For Deimos, these positional uncertainties are on the order of 1.0 km.

5. Discussion

5.1. Comparison with ephemeris predictions

Several teams have made predictions of the Phobos orbit position on the basis of earlier observational data. Full orbit prediction data in SPICE kernel formats are available from the Solar System Dynamics Group at JPL (Jet Propulsion Laboratory) and the orbit analysis group of ESOC (European Space Operation Centre). Specifically, the orbit prediction kernels MAR033_2000-2025.BSP

Table 3. Phobos and Deimos image coordinate measurements.

ID	Image ID	Pho/Dei	Image time	Sample	Line	Error *
1	4130002	P	2004-05-18T08:34:17.052	974.0	539.0	3.0
2	4130003	P	2004-05-18T08:34:19.782	506.0	567.0	20.0
3	4130004	P	2004-05-18T08:34:21.952	73.0	471.0	3.0
4	4130005	P	2004-05-18T08:34:24.687	–428.0	481.0	30.0
5	6490002	P	2004-07-23T12:40:13.577	927.0	511.0	20.0 **
6	6490003	P	2004-07-23T12:40:19.037	395.0	540.0	3.0 **
7	6820001	P	2004-08-01T18:35:02.733	1252.0	–419.0	100.0 ***
8	6820002	P	2004-08-01T18:35:05.453	902.0	–62.0	50.0 ***
9	6820003	P	2004-08-01T18:35:08.183	458.0	–73.0	50.0 ***
10	7150002	P	2004-08-11T00:30:18.173	1458.0	592.0	3.0
11	7150003	P	2004-08-11T00:30:20.358	906.0	604.0	30.0
12	7150005	P	2004-08-11T00:30:24.174	47.0	361.0	50.0
13	7480003	P	2004-08-20T06:25:42.300	276.0	240.0	100.0
14	7480004	P	2004-08-20T06:25:43.940	–144.0	320.0	50.0
15	7480005	P	2004-08-20T06:25:46.115	–661.0	301.0	50.0
16	10640004	P	2004-11-16T14:21:41.141	–188.0	542.0	100.0
17	10640005	P	2004-11-16T14:21:50.946	419.0	549.0	3.0
18	10640006	P	2004-11-16T14:22:00.751	1030.0	574.0	3.0
19	11630002	P	2004-12-14T08:05:08.883	35.0	171.0	3.0 ***
20	11630003	P	2004-12-14T08:05:13.248	433.0	197.0	3.0 ***
21	11630004	P	2004-12-14T08:05:18.149	862.0	215.0	3.0 ***
22	15580005	P	2005-04-03T23:50:09.481	473.0	672.0	3.0
23	15580006	P	2005-04-03T23:50:16.564	1289.0	670.0	50.0
24	15740005	P	2005-04-08T11:20:33.558	448.0	559.0	3.0
25	16070005	P	2005-04-17T17:15:19.487	289.0	701.0	3.0
26	16070006	P	2005-04-17T17:15:27.657	1099.0	695.0	3.0
27	9730001	D	2004-10-22T08:06:02.915	711.0	240.0	3.0
28	9730002	D	2004-10-22T08:06:14.355	510.0	243.0	3.0
29	9730003	D	2004-10-22T08:06:25.811	307.0	243.0	3.0
30	9730004	D	2004-10-22T08:06:37.791	95.0	242.0	3.0
31	10100001	D	2004-11-01T10:15:07.885	706.0	271.0	3.0
32	10100002	D	2004-11-01T10:15:19.340	504.0	276.0	3.0
33	10100003	D	2004-11-01T10:15:30.781	301.0	277.0	3.0
34	10100004	D	2004-11-01T10:15:42.769	90.0	275.0	3.0
35	12220003	D	2004-12-30T19:33:36.845	697.0	189.0	3.0
36	12220004	D	2004-12-30T19:34:06.824	183.0	183.0	3.0

* Estimated one-sigma error in pixels.
** Slewed image (quality of pointing data uncertain).
*** Pointing verified by star measurements.
An identifier in the second row of each table indicates whether the measurements refer to Phobos (P) or Deimos (D). Note that the first four digits of the image ID represent the Mars Express orbit number.

(for the JPL model) and PHOBOS_ESA_2004_2006.BSP/ DEIMOS_ESA_2004_2006.BSP (for the ESOC model) were available. These two prediction models (termed JPL model and ESOC model in the following) differ considerably. According to the ESOC model, both, Phobos and Deimos, have more advanced in their orbits than is predicted by the JPL model. Also, the orientations of the Phobos and Deimos orbits appear to have a relative shift by approx. 3 deg, resulting for example in the effect that at a given time, the out-of-plane components of the predicted Phobos positions differ by varying amounts, +/–10 km in the two models. Laser ranging measurements by MOLA (Mars Orbiting Laser Altimeter) (Banerdt et al. 1999), radiometric measurements of the Phobos shadow by the MOLA receiver (Neumann et al. 2004; Bills et al. 2005), and

Table 4. Phobos and Deimos right ascension and declination, apparent positions #.

ID	Image ID	Pho/Dei	RA, deg	Dec, deg	Error, deg ##
1	4130002	P	87.2271	–3.0065	0.02
2	4130003	P	87.2925	–2.7708	0.02
3	4130004	P	87.2908	–2.5395	0.02
4	4130005	P	87.3506	–2.2850	0.02
5	6490002	P	221.9619	–40.6812	0.02 *
6	6490003	P	221.8039	–41.1716	0.02 *
7	6820001	P	203.2378	–35.3993	0.06
8	6820002	P	202.9440	–35.5029	0.03 **
9	6820003	P	202.8478	–35.7209	0.03 **
10	7150002	P	178.1214	–25.5504	0.02
11	7150003	P	177.9476	–25.7920	0.03
12	7150005	P	177.8050	–26.2397	0.04
13	7480003	P	150.5665	–10.0882	0.06
14	7480004	P	150.3960	–10.2352	0.03
15	7480005	P	150.2351	–10.4536	0.03
16	10640004	P	128.1568	–32.3503	0.05
17	10640005	P	128.1798	–32.6663	0.01
18	10640006	P	128.2142	–32.9839	0.01
19	11630002	P	151.7630	–24.8287	0.01 **
20	11630003	P	151.8753	–25.0101	0.01 **
21	11630004	P	151.9916	–25.2078	0.01 **
22	15580005	P	230.2318	14.9733	0.01
23	15580006	P	230.2428	14.5478	0.03
24	15740005	P	274.4145	–0.6930	0.01
25	16070005	P	267.0145	–0.3927	0.01
26	16070006	P	266.9891	–0.8145	0.01
27	9730001	D	222.7077	–9.4856	0.004
28	9730002	D	222.7234	–9.5893	0.004
29	9730003	D	222.7409	–9.6938	0.004
30	9730004	D	222.7597	–9.8028	0.004
31	10100001	D	219.9086	–4.9287	0.004
32	10100002	D	219.9270	–5.0325	0.004
33	10100003	D	219.9475	–5.1364	0.004
34	10100004	D	219.9705	–5.2441	0.004
35	12220003	D	265.8960	–8.6569	0.004
36	12220004	D	265.9535	–8.9190	0.004

RA and Dec in a spacecraft-centered J2000 frame.
Errors computed from the error model (see details in text and Eq. (1)).
* Slewed images, accuracy of results uncertain.
** Pointing verified by star measurements.

Table 5. Mars Express positions.

ID	Image ID	Pho/Dei	Spacecraft position, km *		
1	4130002	P	5783.70	4873.53	732.04
2	4130003	P	5780.93	4871.64	726.06
3	4130004	P	5778.73	4870.13	721.31
4	4130005	P	5775.95	4868.23	715.33
5	6490002	P	–6496.82	–4703.80	1185.27
6	6490003	P	–6501.12	–4707.70	1196.78
7	6820001	P	–6980.29	–4913.60	1121.50
8	6820002	P	–6982.42	–4915.47	1126.86
9	6820003	P	–6984.56	–4917.33	1132.24
10	7150002	P	–7506.36	–5137.19	1072.26
11	7150003	P	–7508.02	–5138.60	1076.28
12	7150005	P	–7510.91	–5141.05	1083.30
13	7480003	P	–8079.52	–5376.32	1048.80
14	7480004	P	–8080.69	–5377.29	1051.61
15	7480005	P	–8082.24	–5378.57	1055.34
16	10640004	P	–9463.00	–5004.76	4531.66
17	10640005	P	–9452.08	–4999.96	4541.00
18	10640006	P	–9441.14	–4995.14	4550.33
19	11630002	P	–8281.51	–3959.35	3487.78
20	11630003	P	–8275.09	–3956.78	3492.63
21	11630004	P	–8267.89	–3953.88	3498.08
22	15580005	P	–5729.63	–1581.61	–710.17
23	15580006	P	–5720.98	–1580.38	–690.36
24	15740005	P	–5892.27	–1536.35	–1558.23
25	16070005	P	–5549.51	–1376.33	–1432.16
26	16070006	P	–5542.42	–1375.95	–1407.91
27	9730001	D	–11710.76	–6457.10	1897.17
28	9730002	D	–11709.39	–6457.27	1910.44
29	9730003	D	–11707.99	–6457.42	1923.71
30	9730004	D	–11706.50	–6457.56	1937.59
31	10100001	D	–11838.80	–6294.83	1571.81
32	10100002	D	–11836.34	–6294.43	1584.94
33	10100003	D	–11833.85	–6294.01	1598.05
34	10100004	D	–11831.21	–6293.56	1611.78
35	12220003	D	–11273.47	–4582.99	–3152.60
36	12220004	D	–11267.48	–4583.04	–3112.43

* Spacecraft position in Mars-centered equatorial (non-rotating) coordinates.

observations of Phobos and Deimos transits across the solar disk (Bell et al. 2005) have been used to re-assess the position of the two satellites and test the orbit prediction models. Taking the JPL Phobos orbit model as reference, Bills et al. (2005) suggests that the orbit of Phobos has advanced gradually over the time of the MGS mission, from April 1999–July 2004. This is confirmed by the transit observations in March and April 2004 which suggest that Phobos and Deimos were ahead of their predicted position by 11 and 38 km, respectively (Bell et al. 2005). More recently, analysis of HRSC stereo images from the close flyby in orbit 756 in August 2004 (where no SRC images could be obtained) confirmed that the satellite had advanced by approx. 12 km along the orbit (Giese et al. 2005a,b). We have carried out comparisons of all measured Phobos and Deimos positions with both, the JPL and the ESOC prediction model. Our image data consistently show that Phobos has advanced by approx. 12 km with respect to the JPL model, while the predicted Phobos positions in

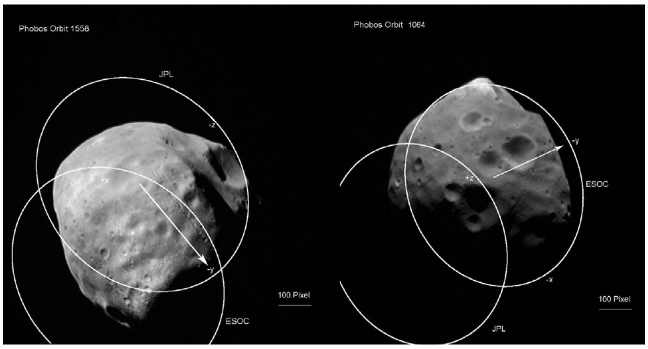

Fig. 4. Phobos and its predicted positions from the JPL and the ESOC model. The direction of the Phobos motion is indicated by the arrow. Note that the spacecraft was near the equatorial plane (*left*) and above the South Pole (*right*) of Phobos, as is indicated by the marked intersection points of the coordinate axes with the reference ellipsoid. Apparently, Phobos is out-of-plane (see left) with respect to the ESOC orbit prediction model. In constrast, Phobos appears to be ahead of its position predicted by the JPL model.

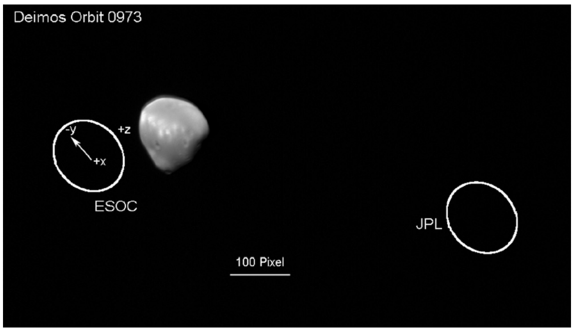

Fig. 5. Deimos and its predicted positions from the JPL and the ESOC model (see Fig. 4 and Table 6 for details).

the across-track directions are off by only small amounts (+/–1 km); hence, our results agree with those of previous Phobos observers. In contrast, while the along-track position of Phobos appears to be in good agreement with predictions by the ESOC model, Phobos appears to be out-of-plane (Fig. 4). All three Deimos observation sequences show that this smaller satellite has advanced by approx. 50 km and is also off across-track with respect to the JPL model. Again, the along-track positions of Deimos appear to be in reasonable agreement (within 5 km) with the ESOC model, while the across-track position components are off (Fig. 5; see Table 6 for details). There are ongoing discussions whether the discrepancy between Phobos observed and predicted positions are due to the positional errors in the early measurements and associated error propagation (Bell et al. 2005) or perhaps due to improper choice of the parameters, e.g., for secular acceleration, in the JPL orbit evolution model (Bills et al. 2005; Lainey et al. 2005; Faehling 2005). On the other hand, no effort has been made (as far as is known to us) to reconcile the puzzling differences in the JPL and the ESOC orbit prediction models. The new positional data reported in this paper may help in the development of up-to-date orbit and error models for Phobos and Deimos.

Table 6. Comparisons of observed and predicted satellite positions.

		JPL model	ESOC model
Phobos	along-track *	+12 km	–2 km
	across-track	+/– 1 km	+/– 8 km
Deimos	along-track *	+ 50 km	–5 km
	across-track	0 km	+/– 18 km

* Positive numbers indicate that the satellite is ahead of the predicted position all numbers with errors +/– 2 km.

5.2. Future work

While the nominal Mars Express mission is scheduled to end by December of this year 2005, plans for an extension of the mission are currently being discussed. The coming Phobos flybys will allow us to make more positional measurements of Phobos in orbit positions, where coverage is currently poor. Also, there will be more opportunities for Deimos observations. It may be worthwhile to use the HRSC images for Phobos position measurements. While the SRC images give us the Phobos 2-D position on the celestial sphere only, the 9 built-in observation channels of HRSC -all pointed in different directions- may allow us to constraint the position of Phobos in 3-D. However, contrary to framing images, the use of the scanner-images for astrometry is not as straightforward, and special measurement software and procedures must be developed. It may also be worthwhile to revisit the image data from the MOC (Mars Orbiting Camera) wide-angle and narrow-angle subsystems on board the Mars Global Surveyor. The images from these cameras are known to contain several hundred observations of the shadow of Phobos (Neumann et al. 2004; Bills & Comstock 2005, see `http://mars.jpl.nasa.gov/mgs/msss/camera/images/11_1_99_phobos/` for examples), which, however, have never been fully analyzed. Contrary to direct observations of Phobos, the position measurements of the satellites shadow are not affected by errors in the spacecraft position or camera pointing. On the other hand, the measurement task is not easy, as the position of the rather diffuse shadow with respect to the morphologic surroundings on the surface of Mars must be determined. From the MGS Phobos shadow data alone, it may be possible to derive a continuous record of the Phobos positions in different orbital phases over the past 8 years.

Acknowledgements. We wish to thank Jorge Diaz del Rio Garcia (ESTEC), Mathias Lauer, and Vicente Companys (ESOC Flight Dynamics) who provided Mars Express orbit and orientation data to us including helpful insights on orbit and attitude data accuracy. We thank the HRSC Experiment Teams at DLR Berlin and Freie Universität Berlin as well as the Mars Express Project Teams at ESTEC and ESOC for their successful planning, acquisition, and processing of HRSC data. We acknowledge the effort of the HRSC Co-Investigator Team members and their associates who have contributed to this investigation. We wish to thank A. Hoffmeister for carrying out the limbfit measurements, and we appreciated helpful comments by Valery Laney on an earlier version of this manuscript. This work was supported by a grant from the Deutsche Forschungsgemeinschaft.

References

Banerdt, W. B., & Neumann, G. A. 1999, Lunar and Planetary Science XXX, 2021

Bell, J. F. F., Fanale, & Cruikshank, D. P. 1993, Chemical and physical properties of the Martian Satellites, in Resources of Near-Earth space, ed. J. Lewis, M. S. Matthews, & M. L. Guerrieri (Tucson: University of Arizona Press)

Bills, B. G., Neumann, G. A., Smith, D. E., & Zuber, M. T. 2005, J. Geophys. Res., 110, E07004

Bills, B. G., & Comstock, R. L. 2005, J. Geophys. Res., 110, E04004

Duxbury, T. C., & Callahan, J. D. 1988, A&A, 201, 169

Duxbury, T. C., & Callahan, J. D. 1989, A&A, 216, 284

Faehling, N. 2005, Rep. on the Implementation and the Verification of the Update of the Martian Moons Orbit Determination, ESA Technical Report, Document No, FDD WO 649, Issue 1.0

Giese, B., Gwinner, K., Oberst, J., et al. 2005a, High resolution mapping of Phobos by the HRSC on Mars Express, First Mars Express Science Conference, Noordwijk, Feb. 21–25

Giese, B., Oberst, J., Scholten, F., et al. 2005b, Ein hochauflsendes digitales Oberflchenmodell des Marsmondes Phobos, Photogrammetrie, Fernerkundung, Geoinformation, submitted

Kolyuka, Y., Tikhonov, V., Ivanov, N., et al. 1991, A&A, 244, 236

Lainey, V., Dehant, V., Rosenblatt, P., Andert, T., & Ptzold, M. 2005, New ephemeris of Phobos and Mars Express close flybys

Morley, T. A. 1989, A&AS, 77, 209

Neukum, G., & the HRSC Co-I Team 2005, The HRSC experiment and scientific results, First Mars Express Science Conference, Noordwijk, Feb. 21–25

Neumann, G. A., Bills, B. G., Smith, D. E., & Zuber, M. T. 2004, Lunar and Planetary Science XXXV, 1820

Oberst, J., Schwarz, G., Behnke, T., et al. 2005, The performance of HRSCs Super Resolution Channel (SRC), First Mars Express Science Conference, Noordwijk, Feb. 21–25

Scholten, F., Gwinner, K., Roatsch, T., et al. 2005, Mars Express HRSC Data Processing - Methods and Operational Aspects, Photogrammetric Engineering and Remote Sensing, in press

Seidelmann, P. K., Abalakin, V. K., Bursa, M., et al. 2002, Celestial Mechanics and Dynamical Astronomy, 82, 83